



Micro grinding 16MnCr5 hardened steel using micro pencil grinding tools with diameters $\sim 50 \mu\text{m}$

Peter A. Arrabiyeh*, Dinesh Setti, Stephan Basten, Benjamin Kirsch, Jan C. Aurich

Institute for Manufacturing Technology and Production Systems, TU Kaiserslautern, 67653 Kaiserslautern, Germany

ARTICLE INFO

Article history:
Available online 10 November 2019

Keywords:
Micro grinding
Electroless plating
Micro pencil grinding tools
Micro machining
ANOVA

ABSTRACT

Micro pencil grinding tools (MPGTs) are micro machining tools that have a huge potential for manufacturing fully micro textured surfaces made out of a broad range of hard and brittle materials, finding use in industries like biomedicine and microelectronics. Due to the flexible manufacturing method used to produce MPGTs - the shape of the tool can be adjusted according to the task at hand. Complex freeform microstructures with various cross sections like dovetails or hemispheres can be produced – cross sections that no other process can produce in brittle materials. MPGTs with diameters $< 50 \mu\text{m}$ however, suffer from a far too short tool life and far too slow achievable feed rates to make the process economical. As part of the tool development process, a parameter study is needed to understand the influence of some of the more important process parameters like feed rate, rotational speed and the tool inclination angle, as well as the grit size. A full factorial experimental design is conducted to determine the importance of each parameter, using an Analysis of Variance (ANOVA) statistical evaluation method. Using the knowledge obtained from the results of this parameter study, optimum parameters were selected for a second case study. Besides increasing the MPGT tool life, the goal was to achieve feed rates beyond 1 mm/min.

© 2019 The Author(s). This is an open access article under the CC BY license (<http://creativecommons.org/licenses/by/4.0/>).

Introduction

Micro components and micro structured surfaces are becoming increasingly relevant for advanced industrial applications; they reduce size and weight of products while integrating more functions in given product size - they help to bridge the gap between the macro and the nano scale [1]. These products found use in various fields such as microfluidics, biomedicine, microelectronics, telecommunications [2] and micro tools [3].

An example of such a miniaturized product is the ongoing development of the lab on a chip technology. A micro electrophoresis chip detects differences in the migration behavior between charged chemical species under the influence of an applied electrical field [4]. These electrophoresis chips are low in cost when compared to bench top devices and can integrate functional elements like reactors or micro pumps – both of these are also used for miniaturized products in the biomedical industry [5]. Other examples of miniaturized products are manufacturing methods for micro tools like micro end mills [3], micro drills [6] and micro pencil grinding tools (MPGTs) [7]. A

number of processes have been used to manufacture micro tools, including: grinding using thin grinding wheels [3], electrical discharge machining (EDM) [8] and laser processing [9]. In turn, these micro tools can be used to produce micro components and micro textured surfaces [3].

In micro structuring operations, other processes like Laser beam machining (LBM) [10], focused ion beam (FIB) [11], etching [12] and μEDM [13] all suffer from an unwanted taper formation with round edges. In addition, each process presents other limitations; FIB is a very expensive process due to long processing times. μEDM suffers from high tool wear and requires an electrically conductive surface [14], it is also prone to cause thermal cracking and to accumulating resolidifying residues in machined structures [15]. Etching as well as micro abrasive blasting requires a prepared chemically inert mask that allows the etching medium to fabricate the desired structure [16]. LBM may cause thermal damage to the machined surface and its sub surface. Micro machining processes are much more flexible, suitable for small batch production, that do not suffer from these form deviations.

Micro end mills made of cemented carbide use a single cutting edge to machine a wide range of ductile materials. This single cutting edge allows micro end mills to machine ductile, soft, smearing materials like titanium alloy and Polymethylmethacrylate (PMMA a

* Corresponding author.

E-mail address: Peter.Arrabiyeh@mv.uni-kl.de (P.A. Arrabiyeh).

transparent thermoplastic) [3] – materials that would immediately clog the chip space on a grinding tool [17]. MPGTs on the other hand are used to machine hard and brittle materials – materials that cannot be machined via drilling or milling [18]. MPGTs are made of a cemented carbide or a steel base body covered with an abrasive layer that consists of super abrasives bound by a metallic layer. These superabrasives are diamonds grits when machining non-ferrous materials or cubic boron nitride (cBN) grits for ferrous [19]. The shape of the base body is directly tied to the shape of the cross-section of the micro structures to be produced, making it possible to produce structures with various cross-sections that cannot be achieved in brittle materials with any other process – shapes like: a hemisphere, a dovetail or a tapered cross-section with a defined angle and sharp edges. Morgan et al. used this unique tool attribute to manufacture MPGTs with a coolant channel for micro holes [20]. Aziz et al. used a different approach by manufacturing a compound micro drilling tool that consists of a flat micro drilling tip and a grinding part with an electroplated abrasive layer [21].

A problem micro pencil grinding tools have is that they provide have a far too low tool life as only few experimental data on their application is available so far. Till now, MPGTs with diameters $<50\ \mu\text{m}$ cannot sustain feed rates high enough to make the process economical for industrial use. A previous study even showed that MPGTs with feed rates of $0.1\ \text{mm}/\text{min}$ have a small probability of losing their abrasive layer at a structure length of $500\ \mu\text{m}$ [22]. Park et al. conducted a parameter study for micro pencil grinding tools (diameter $\sim 100\ \mu\text{m}$), coated with an electroless plating method and diamond grits to machine microstructures in silicon workpieces. The most enduring tool had a grit size of $5\text{--}10\ \mu\text{m}$ and reached a groove length of $650\ \text{mm}$ at a feed rate of $2.4\ \text{mm}/\text{min}$ with a cutting speed of $0.183\ \text{m}/\text{s}$ ($11.3\ \text{m}/\text{min}$) [23]. The study showed potential for industrial use.

This paper will explore the possibility of using MPGTs with diameters of $\sim 50\ \mu\text{m}$ for the machining of hardened 16MnCr5 steel. Two studies will be presented; the first being a case study designed according to a full factorial method to explore the effects of individual parameters: feed rate, rotational speed, grit size and tool inclination angle. The second study utilizes the information received from the first study aiming to increase tool life and feed rate. All studies will be performed applying the previously explored soluble lubricant Sodium Dodecyl Sulfate (SDS) as metal working fluid (MWF) [22].

Experimental setup

Tool manufacturing

As mentioned in the introduction, MPGTs consist of a substrate covered with an abrasive layer. The substrates used in this work are made of ultra-fine grained cemented carbide with a hardness of $1920 \pm 50\ \text{HV}_{30}$ (ISO 3878) [24] and a bending strength of $4800\ \text{N}/\text{mm}^2$. The cemented carbide consists of 92% tungsten carbide and 8% cobalt with a grain size of $0.2\ \mu\text{m}$. The shaft has a diameter of $3.125\ \text{mm}$ and a length of $33\ \text{mm}$. The tool tip is machined using dicing blades to a diameter of $36\ \mu\text{m} \pm 2\ \mu\text{m}$ and a tip length of $150\ \mu\text{m}$ as shown in Fig. 1a. After geometry preparation, the substrate is degreased, etched and primed with a thin nickel layer before electroless plating. The electroless plating solution contains a metal salt that provides the solution with the required metal ions – in this case nickel ions Ni^{+2} and a reducing agent that provides the substrate with the electrons it needs to form a nickel coating on the substrate. Simultaneously, a magnetic stirrer is used to whirl up the solution causing abrasive grits in the solution to move around the container and to collide with the substrate. Due to the constant nickel growth, the grits are embedded into the nickel layer [7].

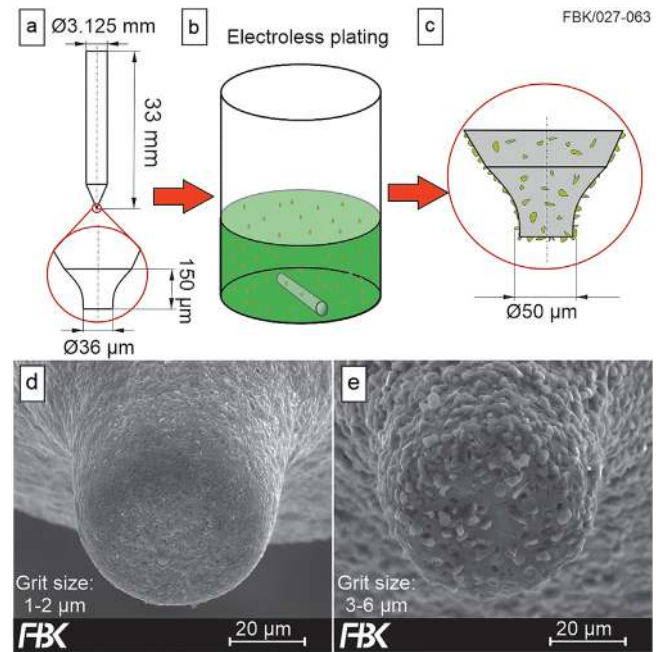


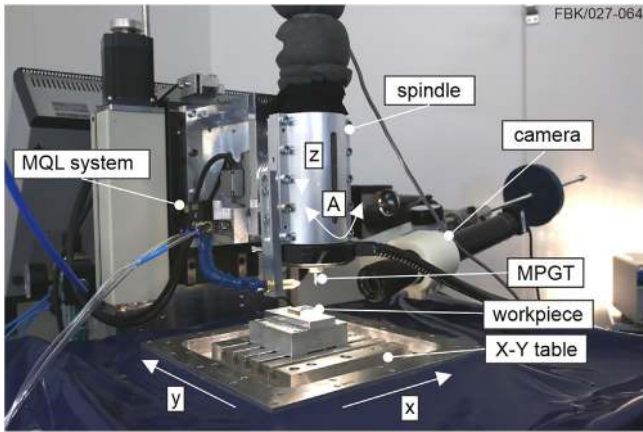
Fig. 1. Manufacturing process of MPGTs: (a) substrate, (b) electroless plating solution, (c) schematic of MPGT, (d) MPGT with $1\text{--}2\ \mu\text{m}$ grit size and (e) MPGT with $3\text{--}6\ \mu\text{m}$ grit size.

Machine tool and instrumentation

A high precision four-axis machine tool that is mounted on top of a granite base that isolates vibrations is used to perform the micro grinding experiments. The machine tool contains a spindle that provides a rotational speed range of $5000\text{--}54,000\ \text{rpm}$ and allows the manual positioning calibration of clamped tools, reducing the reclamping error to values of less than $1\ \mu\text{m}$. The total run-out error (TIR) of the spindle is $3.5\ \mu\text{m}$ at a rotational speed of $30,000\ \text{rpm}$ and $4.5\ \mu\text{m}$ at $50,000\ \text{rpm}$. The spindle is mounted on the Z-axis and is guided by a cross roller bearing. The workpiece is mounted on top of a XY table that is guided by air bearings with a positioning accuracy of $<1\ \mu\text{m}$. The X, Y and Z axis are all powered by a stepper motor and ball screws with a resolution of $2.54\ \text{nm}$. An additional rotational axis is available to achieve the tool inclinations. The rotational axis is powered by a harmonic drive servo system with a resolution of 0.00045° [18]. In addition, a minimum quantity lubrication (MQL) system is used to provide the process with the metal working fluid. Fig. 2 shows the machine tool and its specifications.

Images of MPGTs and their respective 3D structures on the workpiece were captured using a scanning electron microscope (SEM). The structures were analyzed using a confocal microscope (Nanofocus μsurf) with a $60\times$ magnification lens and a numerical aperture of $\text{NA}=0.9$. Stitching algorithms integrated into the measurement device software were used to combine multiple measurements. Missing data points that happen due to finite numerical aperture or due to artifacts on the surfaces were interpolated. Calculations of 2D roughness parameters was limited by the bandwidth of a Gaussian-filter ($l_c=80\ \mu\text{m}$; $l_s=0\ \mu\text{m}$) [25,26].

The quality of the structure was estimated by measuring the mean roughness depth R_z and the arithmetical mean roughness value R_a [27] according to DIN EN ISO 4288. The ISO states that a mean value needs to be calculated from five consecutive $80\ \mu\text{m}$



Four axis machine tool

linear axis: X, Y, Z
 air bearing spindle:
 accuracy: < 1 μm
 travel: 100 mm
 resolution: 2.54 nm
 max spindle speed: 54,000 rpm
 TIR at 30 krpm: < 3.5 μm
 TIR at 50 krpm: < 4.8 μm
 rotational A axis:
 resolution: 0.00045°

Fig. 2. Four-axis machine tool.

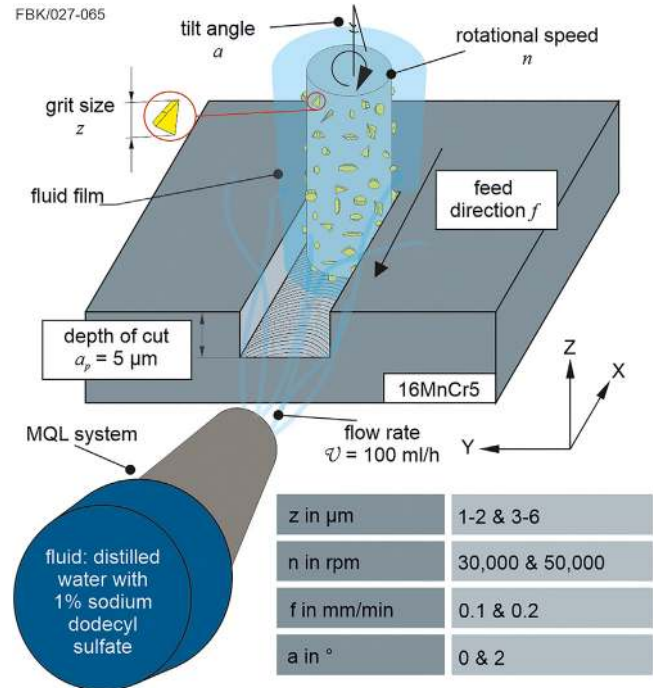


Fig. 3. Process kinematics of micro grinding process.

long segments (in sum 400 μm) were used to calculate the roughness R_{ai} with $i=1, \dots, 5$ of a structure [28]. The first segment is starting at the entry point and is measured at the center of the structure. Structures shorter than 400 μm are still measured to complete the analysis.

Experimental procedure

The workpiece used for the experiments was 16MnCr5 hardened steel with a hardness of 665 ± 15 HV30. Initially, the workpiece was machined with a 3 mm diameter grinding tool, to eliminate all the mounting related errors. The kinematics of the process and the parameter ranges inspected in this study are depicted in Fig. 3.

The tool rotates in clockwise direction around its axis, while the workpiece moves with its defined feed rate towards the tool. The contact point between the tool and workpiece is determined manually by moving the tool towards the workpiece with a slow feed rate. Once contact occurs, the operator observes chip removal with the built-in camera system. The tool is then moved beyond the edge of the workpiece, the depth of cut of 5 μm is adjusted, the metal working fluid is activated and the machining process begins.

The metal working fluid must have a fluid film encasing the MPGT at all times – once the fluid film is interrupted, high tool wear occurs leading to the breakage of abrasive layer [22]. The metal working fluid consists of distilled water with a 1% sodium dodecyl sulfate (SDS) concentration, applied at a constant flow rate of 100 ± 10 ml/h; the selected values are based on preliminary work [22].

The first case study was based on a full factorial experimental design, consisting of four parameters and two levels with each case repeated three times. The case study aimed to identify the effect of process parameters and grit size on tool performance. Grit protrusion, position and concentration were not explored in this paper. However, the same manufacturing parameters were used to

produce MPGTs with the same grit size and each tool was inspected via SEM to ensure that each tool was of the same quality – tools with lumps and other deficiencies were sorted out. Tool performance was evaluated in terms of cutting path and the roughness of the bottom surface in the micro channels. The cutting path in the first case study was limited to 1 mm because previous studies [18,22] showed that unsuitable machining parameters can cause the abrasive layer to break off in the first few hundred micrometers. Table 1 presents the parameters of the performed case study – a total of 16 cases and 48 experiments with a new tool for each.

Analysis of variance

Analysis of variance (ANOVA) is used to create an empirical relation between investigated parameters to determine the significance of process parameters. A test result is statistically

Table 1
 Micro grinding case study.

	(A) Grit size in μm	(B) Feed rate in mm/min	(C) Inclination angle in °	(D) Rotational speed in rpm
Case 1	1–2	0.1	0	30,000
Case 2	3–6	0.1	0	30,000
Case 3	1–2	0.2	0	30,000
Case 4	3–6	0.2	0	30,000
Case 5	1–2	0.1	2	30,000
Case 6	3–6	0.1	2	30,000
Case 7	1–2	0.2	2	30,000
Case 8	3–6	0.2	2	30,000
Case 9	1–2	0.1	0	50,000
Case 10	3–6	0.1	0	50,000
Case 11	1–2	0.2	0	50,000
Case 12	3–6	0.2	0	50,000
Case 13	1–2	0.1	2	50,000
Case 14	3–6	0.1	2	50,000
Case 15	1–2	0.2	2	50,000
Case 16	3–6	0.2	2	50,000

significant if it is deemed unlikely to have occurred by chance. To determine this an evaluation software (Design-Expert) was used to compare the test results with the null hypothesis – that is the absence of a relationship between a factor and an outcome [29]. ANOVA assumes that the null hypothesis is correct until proven otherwise [30]. The probability-value (p-value) determines the probability for the null hypothesis to be untrue. If a set of data reaches significance levels of 95% (p-value = 0.05) and above, it is considered significant. In the present analysis, due to the strong correlation between the selected variables with tool life, it was possible to conduct the analysis at 95% of the confidence interval and a p-value of ≤ 0.05 . However, the same could not be said about the surface roughness as all p-values surpassed the threshold of ≤ 0.05 . This is most likely the result of high initial tool damage for smaller grit sizes as well as adhesions that clog the abrasive layer of the tool upon entry. This is why the threshold was decreased to ≤ 0.1 .

First case study

Wear analysis

As explained in the previous section, tool performance has been identified by evaluating the successful cutting path. Two criteria determined the end of the tool life and the moment it occurred; the first being the delamination of the abrasive layer as depicted in Fig. 4b and an abrupt change in depth of cut that is visible in the machined groove. Only by combining both, the tool and structure images, the exact tool life can be determined - it is common for an MPGT to lose grits during the process. This leads to a small decrease in depth of cut.

A parameter combination was determined as successful if the entire groove is machined without any abrasive layer delamination, as evident from the SEM images of the tools post machining in Fig. 4a and c. Fig. 4a shows a case where MPGTs with a grit size of 1–2 μm were able to machine without failure and Fig. 4b shows a case where the same grit size (1–2 μm) failed to machine the set length at higher rotational speeds and changed tilt angle. This parameter combination proved to be the most difficult one for the tools.

The cases shown in Fig. 4b and c had an increased feed rate, rotational speed and tilt angle, all of which proving to have a negative effect on the tool life. This was further confirmed in the complete evaluation of the case study (Fig. 5).

Using the ANOVA results, main effects and interaction plots were drawn to identify the influence of individual parameters and their interacting effect on the process responses. It is evident from Figs. 5 and 6 that tool life is strongly influenced by grit size, rotational speed and their interaction. As the size of grits plays a very significant role, effects of other factors are negligible when the size of the grits is larger.

Eq. (1) shows that at higher rotational speeds n the maximum uncut chip thickness value $h_{cu,max}$ decreases. In conventional machining processes, the chip thickness value has to be higher than the minimum chip thickness value, otherwise rubbing and ploughing actions are promoted, which could lead to higher temperatures in the contact zone and ultimately in abrasive layer failure. Hence, the reason for tool failure - at least for the 1–2 μm grit size - could be attributed to the reduced chip thickness values at higher rotational speeds. Under the same conditions, tools with larger grits can produce the grooves successfully within the defined length. The much lower number of cutting edges increases the probability of a single grit reaching a high uncut chip thickness value, decreasing the ploughing and rubbing actions. Evidently, MPGTs with a grit size of 3–6 μm were able to machine a 1 mm long groove successfully in all the conditions without failure. In spite of this, MPGTs with larger grit sizes seem to have much

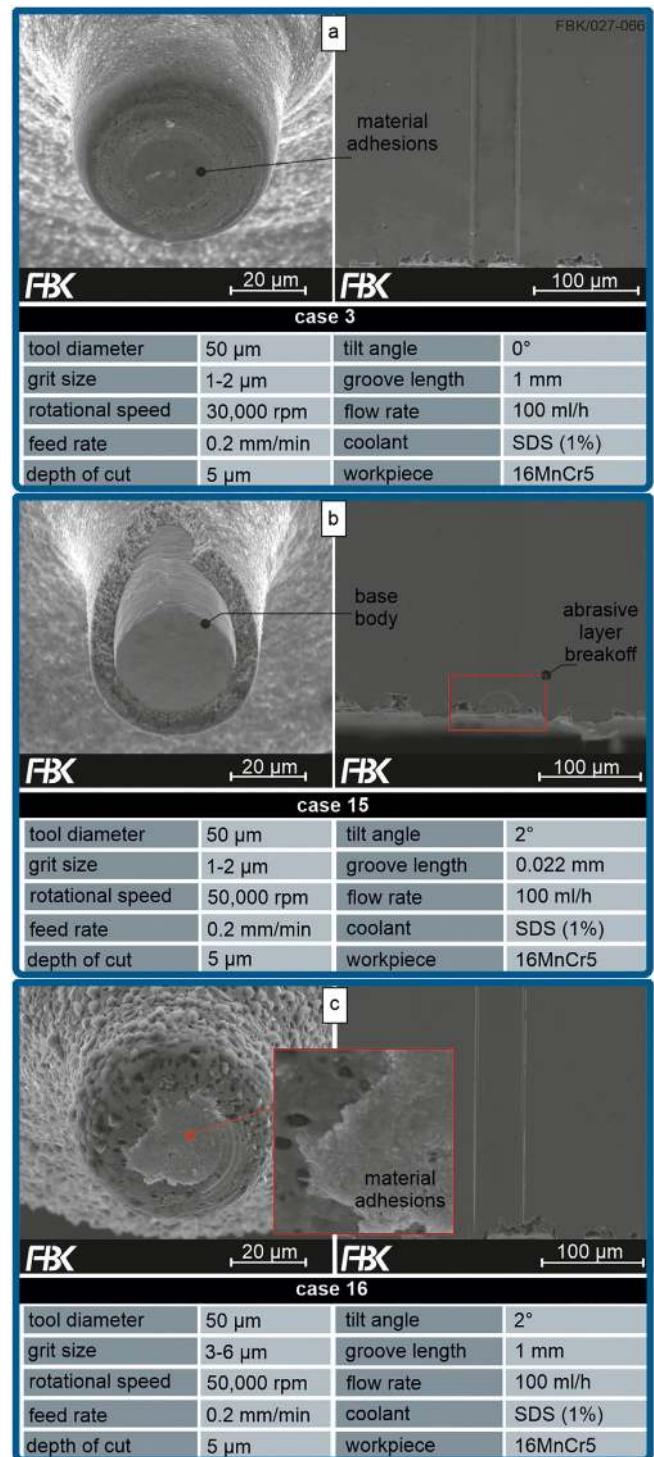


Fig. 4. Post-process images of MPGT and machined structure for the cases (a) 3, (b) 15 and (c) 16.

adhesions, adhering to the tool bottom (as illustrated in Fig. 4c). Material adhesion was originating from the center of the tools, causing the clogging of the abrasive layer. These adhesions occur due to short term friction welding processes of accumulating chips [31]. Adhesions that clog the chip space increase friction, process temperatures, and process forces; ultimately increasing the wear of the tool by breaking out single grits or even entire grit populations [17]. Higher rotational speeds also increase clogging

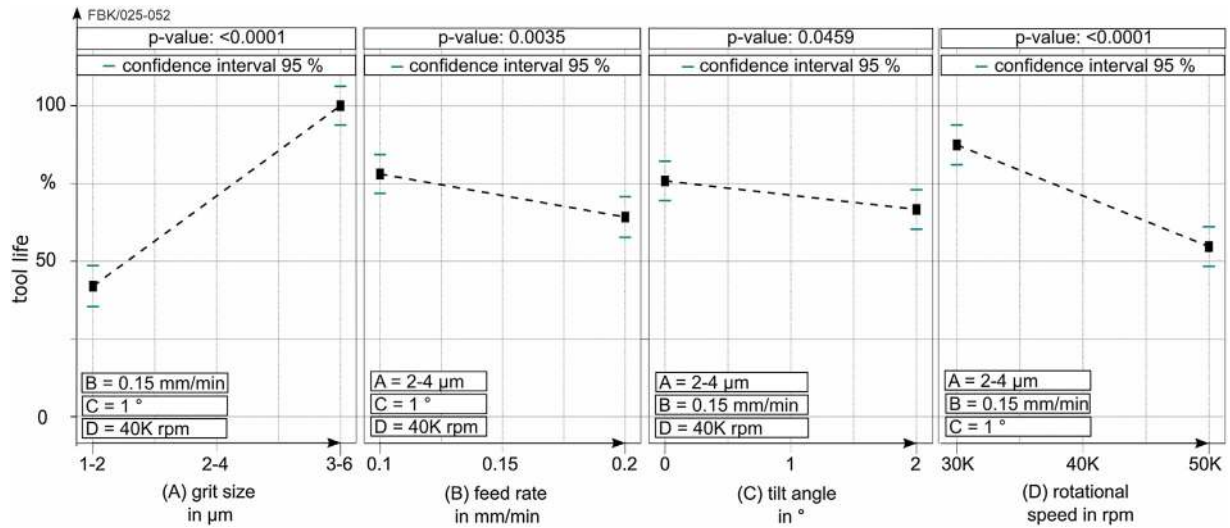


Fig. 5. Main effects of the four investigated parameters on tool life (in percent of 1 mm groves).

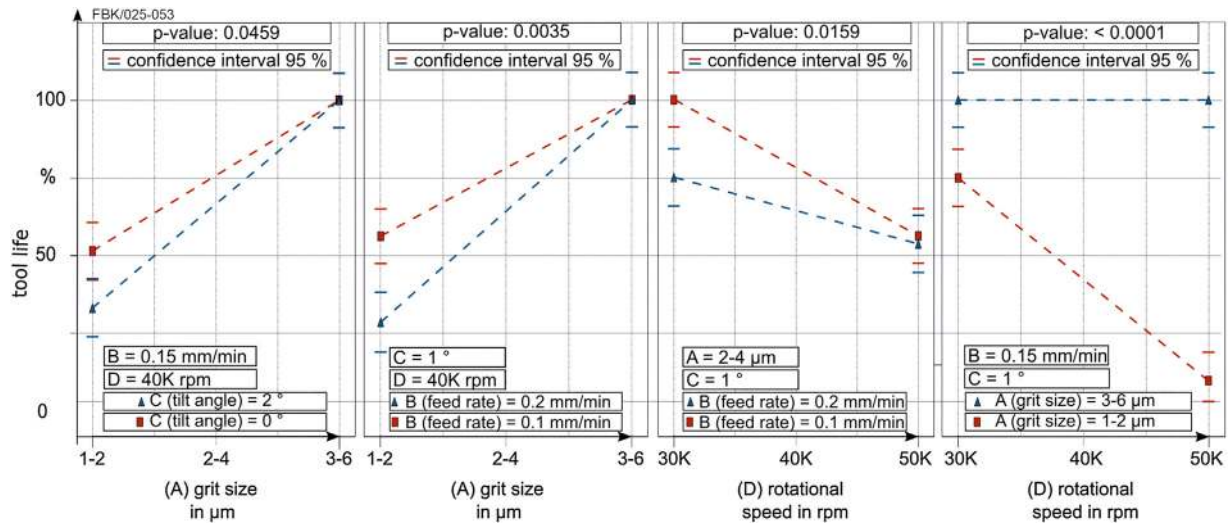


Fig. 6. Effects of interactions of grit size (A), feed rate (B), tilt angle (C) and rotational speed (D) on tool life (in percent of 1 mm groves).

due to increased temperatures and pronounced rubbing and ploughing actions [31].

$$\frac{h_{cu,max}}{n} \propto V_f \quad (1)$$

In conclusion, the grit size proved to be the most influential parameter as all MPGTs with a grit size of 3–6 μm managed to machine the 1 mm long groove in its entirety. An increase in rotational speed proved to reduce tool life, especially for the lower grit size.

Groove analysis

The characteristics of the micro structures are unique for each MPGT and can only be replicated with great difficulty. They are influenced by the MPGTs grit concentration, protrusion, and positioning as well as intermittent material adhesions.

Depending on the position and protrusion of each grit at the bottom surface of the MPGT, unique, so called substructures are formed at the bottom of the micro structures. As demonstrated in Fig. 7b, these substructures can easily reach heights of a few micrometers and can therefore influence the functionality of the overall microstructure. In (a) a schematic, showing an MPGT and a microstructure is presented. In this theoretical case, an MPGT that has the largest grit protrusions at the center of the tool, is used in a machining experiment. Ignoring the machine tools run-out, vibrations and re-clamping errors, the microstructure received would take a shape according to the grit distribution. The grits cutting edge distance from the pivot of the tool (dimensions c and d in Fig. 7a) and difference in grit protrusions (dimensions a and b in Fig. 7a) would define the substructure widths and heights. In addition to the grits, the aforementioned adhesions at the tool bottom, as exemplarily shown in Fig. 7c), contribute to the formation of substructures. Substructures resulting from these adhesions, which act like built-up edges,

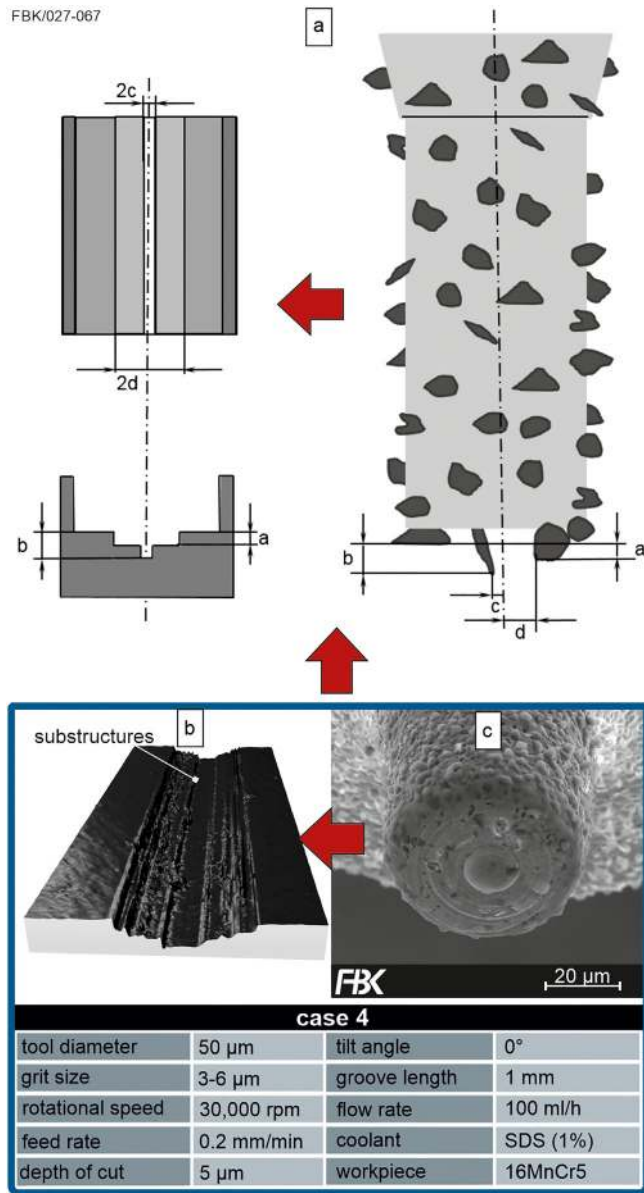


Fig. 7. (a) Schematic of an MPGT and machined micro structure, (b) confocal microscopic image of a micro structure in case 4, (c) MPGT post machining.

may not form at the beginning of the machining process, but are likely to occur later.

Fig. 8 shows confocal microscopic images of cases 1, 2, 12 and 16, presenting distinct differences, related to parameter variations. The representative images of cases 1 and 2 show that the grit size has little to no influence on the structure – provided of course that the same machining conditions are used and the abrasive layer is not damaged during the process. Damage to the abrasive layer occurs much more often to MPGTs with smaller grit sizes, which is why MPGTs with larger grit sizes deliver microstructures with more consistent roughness values. A significant improvement in structure quality was documented for cases 12 and 16, cases in which both the rotational speed and the feed rate have been increased simultaneously. In case 16 the tilt angle was also changed which is reflected by the orientation of the grinding marks (Fig. 8).

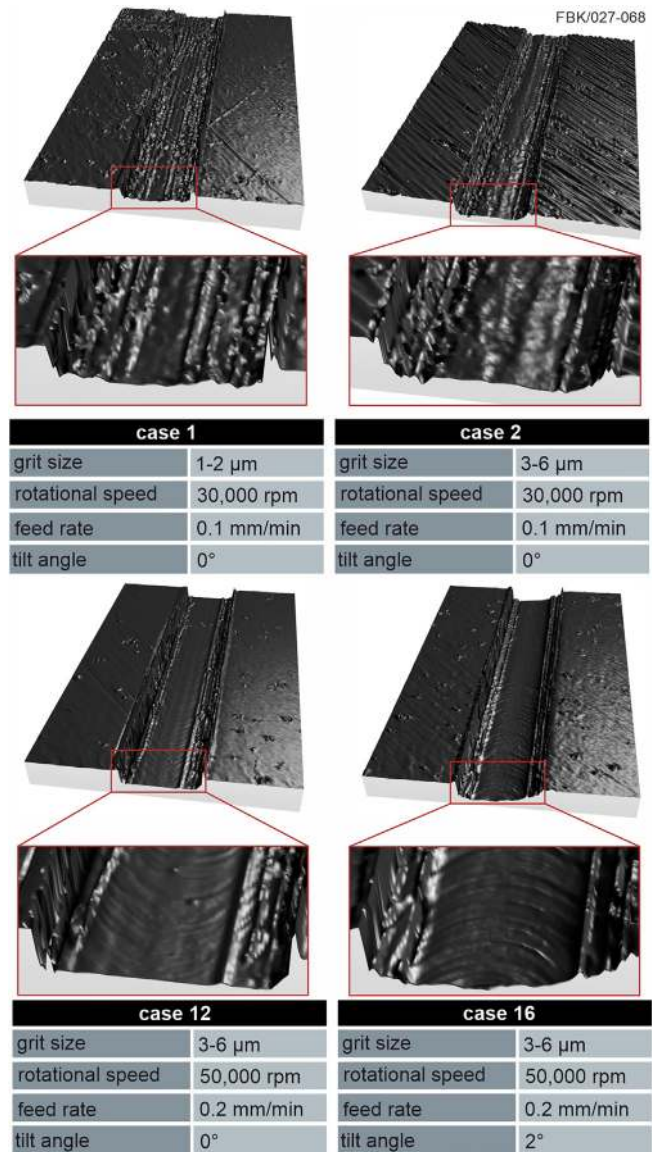


Fig. 8. Confocal microscopic images of machined structures: case 1, case 2, case 12 and case 16.

In the case of surface roughness ANOVA showed that all factors had similar p-values, except for the grit size, which had a p-value of 0.64. This is why the grit size was taken out of the calculations, conducted by the evaluation program and hence is why Fig. 9 only shows the effects of the rotational speed, tilt angle and feed rates as well as their interactions together. As mentioned in Section “Wear analysis”, chip adhesion at the tool bottom significantly effects the surface quality, which is very difficult to predict in terms of process kinematics. Especially good results occurred when simultaneously increasing rotational speed and feed rate as well as rotational speed and tilt angle.

Second case study

Micro grinding case study and tool description

Using the information obtained from the preliminary experiments presented in Section “First case study”, three additional

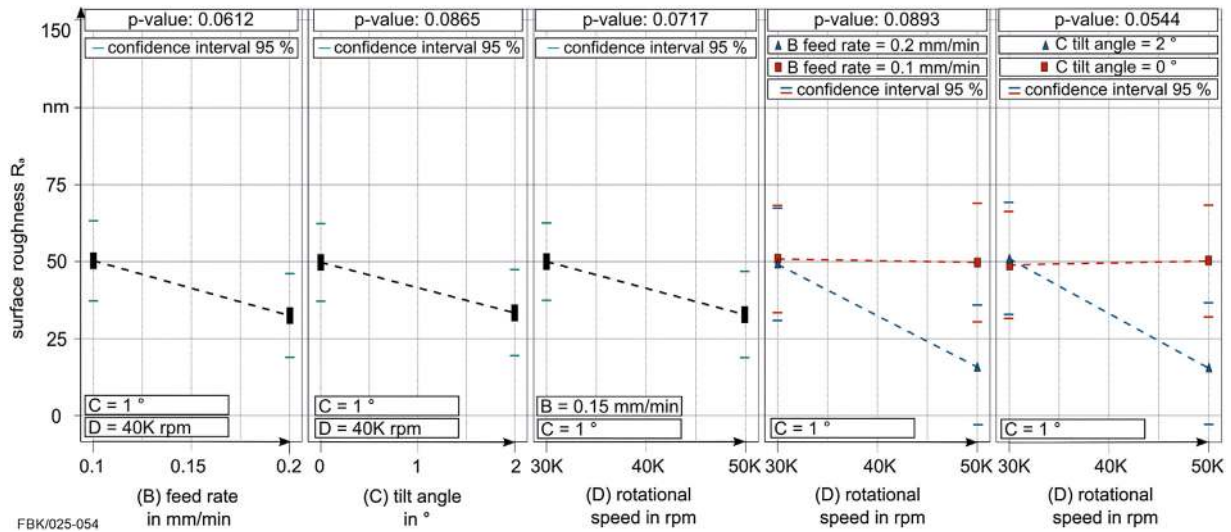


Fig. 9. Effects of rotational speed (D), feed rate (B) and tilt angle (C) on surface roughness and their interactions.

Table 2
Second micro grinding case study.

	Grit size in μm	Feed rate in mm/min	Tilt angle in $^\circ$	Rotational speed in rpm
Case 22	5–10	1	0	30,000
Case 23	5–10	2	0	30,000
Case 24	5–10	4	0	30,000

cases were conducted to demonstrate the tool life at higher feed rates (≥ 1 mm/min). According to the diagrams in Fig. 5, a rotational speed of 30,000 rpm, a tilt angle of 0° and grit size of $3\text{--}6\ \mu\text{m}$ showed the highest tool life, with the grit size having the highest influence. The grit size was increased to $5\text{--}10\ \mu\text{m}$ in order to achieve a better tool performance. Despite the improved surface finish achieved with higher rotational speeds, it was decided to use the lower rotational speed in favor of a longer tool life. Table 2 shows the kinematic conditions for the additional experiments. Each case was conducted at least two times. Fig. 10 shows an MPGT with a grit size of $5\text{--}10\ \mu\text{m}$.

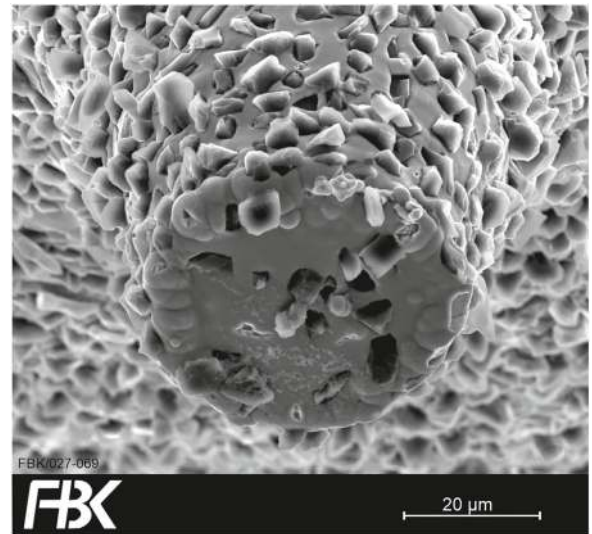


Fig. 10. Micro pencil grinding tool with grit size $5\text{--}10\ \mu\text{m}$.

Wear and structure analysis

SEM images of the tools showed high quantities of material adhesions on the bottom surface of the tool as can be seen in Fig. 11 (same tool as in Fig. 10). The tool machined the structure shown in Fig. 14. A new porous layer made of steel chips covers most of the grits; a friction stir welding is assumed to be the cause for the adhesion: energy dispersive X-ray (EDX) analysis showed a high iron concentration on the bottom surface with the highest concentration found in the area marked in Fig. 11. Adhesions cause the cutting tool to blunt and it contaminates the machined surfaces [32]. A method to decrease adhesions is required in future research.

Fig. 12 shows three structures machined with different feed rates, demonstrating the burr formation progression with increasing feed rate. As described above, the bottom of the structure varies according to grit position, grit protrusion, and grit concentration. For longer structure lengths, the bottom of the

structure may vary in the same structure due to adhesions, grit break outs or abrasive wear.

The largest cutting path achieved was measured to 35.4 mm, at a feed rate of 2 mm/min. The lowest roughness value R_a was measured at 18.9 nm for a feed rate of 4 mm/min; however, the cutting path of this tool was measured at 0.14 mm. Fig. 13 shows the results obtained from this experimental series.

Both the tool life and the achievable feed rates improved after adjusting the grit size, the tilt angle and the rotational speed. To prove the processes capabilities in machining closed structures, the shape of a house was machined with a feed rate of 2 mm/min – depicted in Fig. 14. The structure length is 4.215 mm and is machined without interruption. The shape of a house presents the challenge that the tool changes machining direction upon finishing each line; covering all eight, straight and diagonal directions (see Fig. 14).

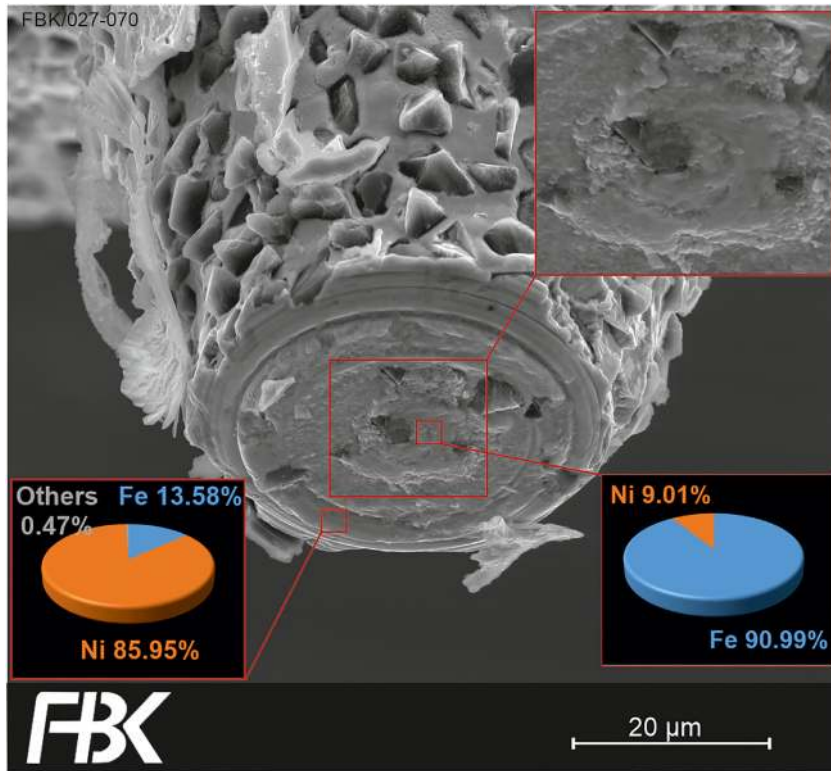


Fig. 11. Tool wear mechanisms.

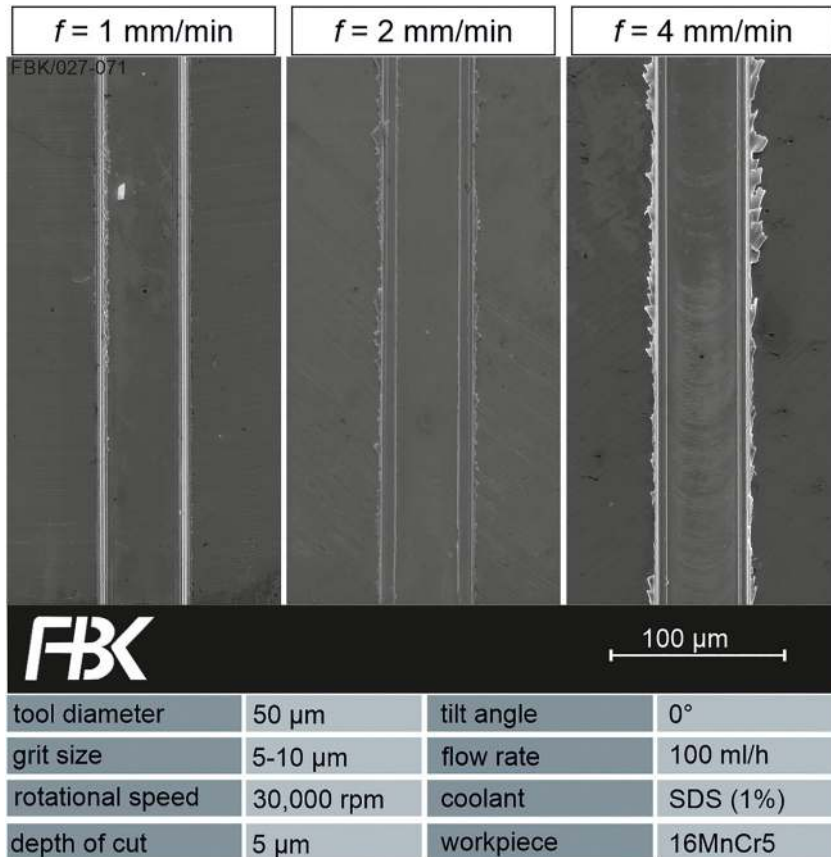


Fig. 12. Burr formation with different feed rates.

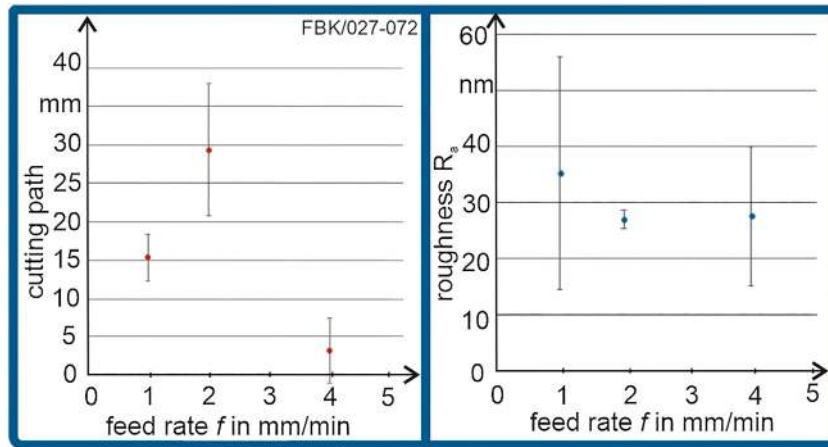


Fig. 13. Diagrams of cutting path and roughness value R_a over feed rate.

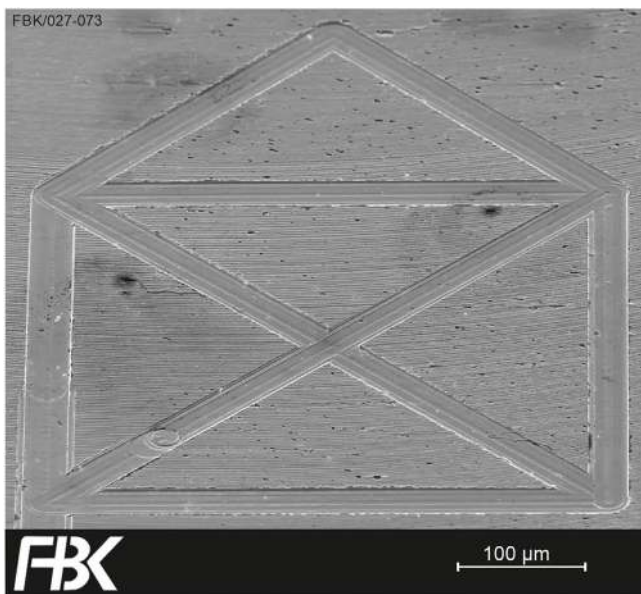


Fig. 14. Structure in the shape of a house.

Conclusions and outlook

Micro pencil grinding tools (MPGTs) with diameters smaller than $50\ \mu\text{m}$ suffer from a low tool life and low achievable feed rates. Two case studies have been conducted to analyze possibilities to optimize the process. The first was a full factorial experimental design and conducted to determine the importance of rotational speed, grit size and the tilt angle of the tool, using an Analysis of Variance (ANOVA) evaluation method. Rotational speeds of 30,000 rpm and 50,000 rpm, grit sizes of $1\text{--}2\ \mu\text{m}$ and $3\text{--}6\ \mu\text{m}$, feed rates of 0.1 mm/min and 0.2 mm/min as well as a tilt angle of 2° were inspected, adding up to 48 experiments in 16 cases. In order to test the validity of selected parameters, 1 mm long grooves were machined in 16MnCr5 (665 HV30) at a depth of cut of $5\ \mu\text{m}$. The results showed that an increase in rotational speed and tilt angle improve the quality of machined structures, but reduce the tool life. An increase in grit size showed only minor influence on the surface quality but increased the tool life dramatically. Every tool coated with a $3\text{--}6\ \mu\text{m}$ grit size achieved

to complete the 1 mm groove length without failure. Grit size proved to be the most important parameter concerning tool life.

Based on the results of the first case study, a second case study was conducted, using MPGTs with a grit size of $5\text{--}10\ \mu\text{m}$ and a rotational speed of 30,000 rpm. The MPGTs were tested with feed rates of 1 mm/min, 2 mm/min and 4 mm/min until failure. A groove length of 35.4 mm was machined using the feed rate of 2 mm/min. Both the tool life and the achievable feed rates increased tremendously. However, energy dispersive X-ray (EDX) analysis showed a high iron concentration at the bottom surface of the MPGTs with the highest concentrations gathering at the pivot. This is especially a problem when machining materials that are more ductile. Further improvements in both tool life and surface roughness might be possible if a solution to the iron adhesions problem is found. In addition, a better adhesion between the abrasive layer and the base body of MPGTs can be achieved by further improving the coating procedure.

Declaration of Competing Interest

The authors declare that they have no known competing financial interests or personal relationships that could have appeared to influence the work reported in this paper.

Acknowledgement

This research was funded by the Deutsche Forschungsgemeinschaft (DFG, German Research Foundation) – Projektnummer 172116086 – SFB 926.

References

- [1] Feng, J., 2010, *Microgrinding of Ceramic Materials*.
- [2] Pratap, A., Patra, K., Dyakonov, A.A., 2016, Manufacturing Miniature Products by Micro-Grinding: A Review. *Procedia Engineering*, 150:969–974.
- [3] Aurich, J.C., Reichenbach, I.G., Schüler, G.M., 2012, Manufacture and application of Ultra-Small Micro End Mills. *CIRP Annals*, 61/1: 83–86.
- [4] Schlaumann, S., Wensink, H., Schasfoort, R., Elwenspoek, M., Berg, A-v-d, 2001, Powder-Blasting Technology as an Alternative Tool for Microfabrication of Capillary Electrophoresis Chips with Integrated Conductivity Sensors. *Institute of Physics*.
- [5] Tiggelaar, R.M., Veenstra, T.T., Sanders, R.G.P., Berenschot, E., Gardeniers, H., Elwenspoek, M., et al., 2003, Analysis Systems for the Detection of Ammonia Based on Micromachined Components Modular Hybrid Versus Monolithic Integrated Approach. *Sensors and Actuators B: Chemical*, 92/1–2: 25–36.
- [6] Butler-Smith, P., Warhanek, M., Axinte, D., Fay, M., Bucourt, J.-F., Ragueneau, R., et al., 2016, The Influences of Pulsed-Laser-Ablation and Electro-Discharge-

- Grinding Processes on the Cutting Performances of Polycrystalline Diamond Micro-Drills. *CIRP Annals*, 65/1: 105–108.
- [7] Arrabiyeh, P.A., Kirsch, B., Aurich, J.C., 2017, Development of Micro Pencil Grinding Tools Via an Electroless Plating Process. *Journal of Micro and Nano-Manufacturing*, 5/1. 011002-1–011002-6.
- [8] Egashira, K., Hosono, S., Takemoto, S., Masao, Y., 2011, Fabrication and Cutting Performance of Cemented Tungsten Carbide Micro-Cutting Tools. *Precision Engineering*, 35/4: 547–553.
- [9] Onikura, H., Ohnishi, O., Take, Y., Kobayashi, A., 2000, Fabrication of Micro Carbide Tools by Ultrasonic Vibration Grinding. *CIRP Annals*, 49/1: 257–260.
- [10] Dubey, A.K., Yadava, V., 2008, Laser Beam Machining—A Review. *International Journal of Machine Tools and Manufacture*, 48/6: 609–628.
- [11] Reyntjens, S., Puers, R., 2001, A Review of Focused Ion Beam Applications in Microsystem Technology. *Journal of Micromechanics and Microengineering*, 11/4: 287–300.
- [12] Saito, Y., Okamoto, S., Miki, A., Inomata, H., Hidaka, T., Kasai, H., 2008, Fabrication of Micro-Structure on Glass Surface Using Micro-Indentation and Wet Etching Process. *Applied Surface Science*, 254/22: 7243–7249.
- [13] Mahendran, S., Devarajan, R., Nagarajan, T., Majdi, A., 2010, Review of Micro-EDM. *Proceedings of the International Multiconference of Engineers and Computer Scientists*, .
- [14] Yu, Z.Y., Zhang, Y., Li, J., Luan, J., Zhao, F., Guo, D., 2009, High Aspect Ratio Micro-Hole Drilling Aided with Ultrasonic Vibration and Planetary Movement of Electrode by Micro-EDM. *CIRP Annals*, 58/1: 213–216.
- [15] Ekmekci, B., 2007, Residual Stresses and White Layer in Electric Discharge Machining (EDM). *Applied Surface Science*, 253/23: 9234–9240.
- [16] Wensink, H., 2002, Fabrication of Microstructures by Powder Blasting. University of Twente [Host], Enschede.
- [17] Klocke, F., 2009, *Manufacturing Processes 2: Grinding, Honing, Lapping*. Springer-Verlag Berlin Heidelberg, Berlin, Heidelberg.
- [18] Kirsch, B., Bohley, M., Arrabiyeh, P.A., Aurich, J.C., 2017, Application of Ultra-Small Micro Grinding and Micro Milling Tools: Possibilities and Limitations. *Micromachines*, 8/9: 261.
- [19] Hoffmeister, H.-W., Hlavac, M., 2002, Schleifen von Mikrostrukturen. *Tagungsband des 10. Feinbearbeitungskolloquiums in Braunschweig, 2002:7. 1–7.24.*
- [20] Morgan, C., Vallance, R.R., Marsh, E.R., 2006, Improved Finish and Form in Blind Holes Using Polycrystalline Diamond Micro Tools. *International Conference on Micromanufacturing 1*, .
- [21] Aziz, M., OHNISHI, O., ONIKURA, H., 2012, Innovative Micro Hole Machining with Minimum Burr Formation by the Use of Newly Developed Micro Compound Tool. *Journal of Manufacturing Processes*, 14/3: 224–232.
- [22] Arrabiyeh, P.A., Bohley, M., Ströer, F., Kirsch, B., Seewig, J., Aurich, J.C., 2017, Experimental Analysis for the Use of Sodium Dodecyl Sulfate as a Soluble Metal Cutting Fluid for Micromachining with Electroless-Plated Micropencil Grinding Tools. *Inventions*, 2/29.
- [23] Park, H.-K., ONIKURA, H., OHNISHI, O., Sharifuddin, A., 2010, Development of Micro-Diamond Tools Through Electroless Composite Plating and Investigation into Micro-Machining Characteristics. *Precision Engineering*, 34/3: 376–386.
- [24] DIN EN ISO 3878. 1991, DIN EN ISO 3878 Hardmetals; Vickers Hardness Test (3878)..
- [25] DIN EN ISO 16610-21. 2012, DIN EN ISO 16610-21: Geometrical Product Specifications (GPS) – Filtration – Part 21: Linear Profile Filters. 2013 ed Gaussian filters
- [26] DIN EN ISO 11562:1998-09. 1997, DIN EN ISO 11562: Geometrical Product Specifications (GPS) – Surface Texture: Profile Method – Metrological Characteristics of Phase Correct Filters..
- [27] DIN EN ISO 4287:2010-07. 2009, Geometrical Product Specifications (GPS) – Surface Texture: Profile Method – Terms, Definitions and Surface Texture Parameters..
- [28] DIN EN ISO 4288:1998-08. 1997, Geometrical Product Specifications (GPS) – Surface Texture: Profile Method – Rules and Procedures for the Assessment of Surface Texture..
- [29] Wasserstein, R.L., Lazar, N.A., 2016, The ASA's Statement on p-Values: Context, Process, and Purpose. *The American Statistician*, 70/2: 129–133.
- [30] Ratnam, C., Arun Vikram, K., Ben, B.S., Murthy, B.S.N., 2016, Process Monitoring and Effects of Process Parameters on Responses in Turn-Milling Operations Based on SN Ratio and ANOVA. *Measurement*, 94:221–232.
- [31] Lauer-Schmaltz, H., König, W., 1980, Phenomenon of Wheel Loading Mechanisms in Grinding. *CIRP Annals*, 29/1: 201–206.
- [32] Lin, J.-W., Cheng, M.-H., 2014, Investigation of Chipping and Wear of Silicon Wafer Dicing. *Journal of Manufacturing Processes*, 16/3: 373–378.